Internal Waves and Bedforms

5

Hans van Haren

Abstract

The physics of internal waves in the density-stratified deep sea is reviewed with the aim of understanding the waves' potential effects on undular bedforms, 'sediment waves', at the seafloor. Such bedforms occur mainly on continental slopes. Sloping topography is also a prerequisite for internal wave breaking, which is the dominant process for sediment resuspension in the deep sea. Internal and sediment waves have common horizontal length scales. They differ in vertical length scale and, foremost, in propagation velocity and age.

Keywords

Internal waves • Sediment waves • Sloping topography • Turbulent bores • Inertial motions

5.1 Introduction

As seas and oceans are basically heated from above, they are stably stratified in density because warm water is less dense than cold water. The heat stored as potential energy near the surface is transported into the deep sea by means of mechanical turbulent mixing. The main supply of kinetic energy comes from tides, and from inertial motions following the passage of atmospheric disturbances on the rotating Earth. The former dominate in most oceans, the latter in the Mediterranean Sea. The fact that as little as 1/30,000 of the potential energy is needed in kinetic energy to provide sufficient mixing to keep the deep-sea stratified (Munk and Wunsch 1998) shows the importance of ocean tides and inertial motions.

The same density stratification supports freely propagating 'internal waves' at frequencies between inertial frequency $f = 2\Omega\sin\varphi$ at latitude φ, where Ω is the Earth's angular velocity, and buoyancy frequency $N = (-g/\rho \cdot d\rho/dz)^{1/2}$ plus

H. van Haren (✉)
Royal Netherlands Institute for Sea Research (NIOZ), P.O. Box 591790 AB Den Burg, the Netherlands
e-mail: hans.van.haren@nioz.nl

© Springer International Publishing Switzerland 2017
J. Guillén et al. (eds.), *Atlas of Bedforms in the Western Mediterranean*,
DOI 10.1007/978-3-319-33940-5_5

compressibility correction, where g is the acceleration of gravity and ρ the density. In contrast with surface (wind) waves, internal waves are essentially three-dimensional, as only N-waves propagate strictly along density interfaces with their velocity directed vertically, while pure inertial motions are horizontal. As a result, waves at all frequencies (σ) in the range $f < \sigma < N$ propagate at a particular angle to the vertical (e.g., LeBlond and Mysak 1978). Thus, depending on local values of f and N, internal waves are generated and break at particular slope sections of the bottom topography. This fact associates particular sections of underwater seamounts and continental slopes with relatively strong turbulent mixing.

Undulating bedforms rather than sliding structures are also observed uniquely above particular slopes, mostly seaward of river outflow. Examples of such 'sediment waves' in prodeltas of river outflows above continental slope sections are given in Urgeles et al. (2011) and in various chapters of this book. Although the mechanisms of their formation, development or maintenance are not well understood, it is tempting to compare physical processes of internal wave generation and, more importantly, wave breaking, with the formation of sediment waves. In this chapter, properties of physical and geological processes are reviewed and some dedicated observational setups for the investigation of internal wave impact on sediment wave formation are discussed.

5.2 Internal Wave Impact on Sediment

While in shallow seas—say less deep than 50 m—the sediment is mainly reworked by the impact of surface wind waves and (tidal) currents through bottom friction in the lower 5–10 m, at greater depths these effects are less important. Above the continental slope, boundary currents like the Northern Current in the NW Mediterranean may be responsible for some friction when they reach the bottom. However, most resuspension of sediment is observed to occur during the relatively short moments of breaking of shoaling internal waves (Hosegood et al. 2004). Thereby, the internal waves deform nonlinearly from their sinusoidal shape in the interior to create an upslope-moving, vigorously turbulent bore (Vlasenko and Hutter 2002; Klymak and Moum 2003). Including their pre-frontal sharpening, the bores account for 60 % of the turbulence generated in a tidal cycle within half an hour (van Haren and Gostiaux 2012). The sediment is swept up by 0.05–0.15 m s^{-1} vertical currents of the 10- to 60-m-high bores (examples in Figs. 5.1 and 5.2), as in an atmospheric dust storm. This phenomenon results in nepheloid layers dispersed along isopycnals in the ocean interior (e.g., Armi 1978; Cacchione and Drake 1986; McPhee-Shaw and Kunze 2002).

It has been suggested that nepheloid layers are associated with bottom slopes (β) that 'critically' match the internal

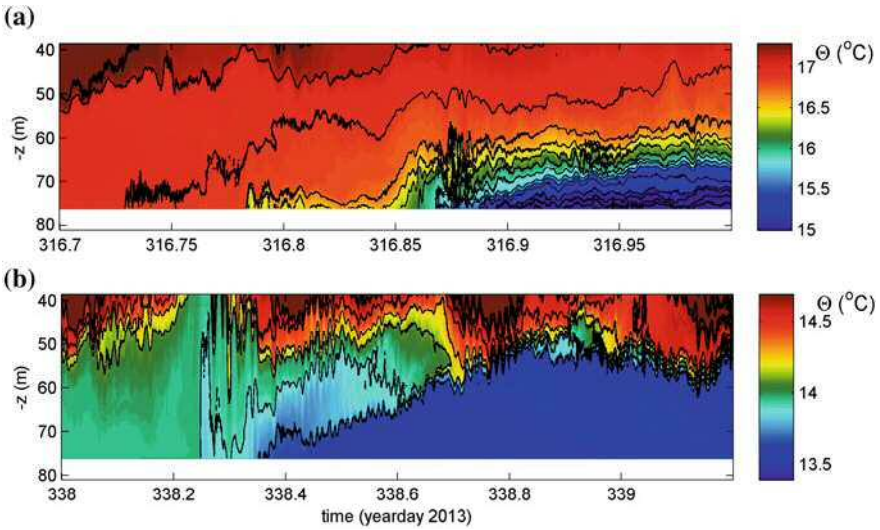

Fig. 5.1 Two examples of high-frequency internal waves in the Llobregat prodelta (Barcelona harbour entrance buoy), observed using high-resolution NIOZ temperature sensors during the autumn of 2013 (van Haren, Guillén, Puig, unpublished results). Contour interval is 0.2 °C. **a** 7 h time-window showing a near-bottom bore moving upslope, while it mixes with overlying water (e.g. day 316.87 between 60 and 75 m) and generates high-frequency internal waves. **b** Three weeks later, note the cooler temperatures and the time-window of 28 h, also showing a cold-water bore but with high-frequency internal waves at an interface 20–30 m above the bottom

wave slope $\alpha = \arcsin(\sigma^2 - f^2)/(N^2 - f^2) \equiv \beta$ (see e.g. Lamb 2014 for geometry of super- and sub-critical bottom slopes for internal wave beams). This association may be related to the generation site of, e.g., internal tides at which the near-bottom (<5 m) shear appears to be high as modelled by Zhang et al. (2008). In their model, internal wave breaking is not resolved. However, ocean observations confirm that most vigorous internal wave breaking, and associated sediment resuspension transported much higher up to about 50 m above the bottom, does not occur above critical slopes, but rather on steep slopes that are supercritical $\beta > \alpha$ for semidiurnal lunar tides (Hosegood et al. 2004; van Haren et al. 2015). At such slopes internal tides reflect back into the interior (Lamb 2014) and higher frequency internal waves may be critical. There, the average turbulent kinetic energy dissipation is found to be 100 times greater than at subcritical slopes and in the ocean interior. Furthermore, turbulent bores have been associated with tidal, inertial and sub-inertial 'carrier' waves. The latter two are not considered freely propagating internal waves in the traditional approximation because, e.g., at f, $\alpha = 0$ in theory. In practice, the inertial band has a finite width of approximately [0.95f, 1.05f] and near-inertial internal waves in modulation with the Northern Current are observed to occasionally create bores in the Gulf of Valencia (van Haren et al. 2013). In general in the Mediterranean, tides are very weak with a few exceptions, e.g., near Gibraltar and in the northern Adriatic.

Although to my knowledge a precise relation between bedform occurrence and slope angle is presently lacking, it seems that sediment waves mainly occur on the deep-sea side of the steepest part of a continental slope (see examples in Verdicchio and Trincardi 2006; Puig et al. 2007; Urgeles et al. 2011; Ribó et al. 2016). Typical amplitudes are 1–10 m in the vertical, with 100- to 1000-m horizontal wave lengths. The former are one to two orders of magnitude smaller than those of internal wave (bores). The latter, however, match the length scales of internal waves, which vary between several tens of metres at N and about 1 km at f (and tidal frequencies) (LeBlond and Mysak 1978).

5.3 Observational Setup

Variations in internal wave breaking and sediment resuspension are best studied using underwater moored instrumentation that is left unattended for at least a month to build-up some statistics with the varying low-frequency motions. Sediment traps and optical backscatter devices may be attached to the mooring line to monitor variations in suspended materials. Preferably, multiple instruments should be attached to the typically 100-m longline in the vertical, together with multiple current meters. To investigate internal wave breaking in detail and to quantify the turbulence dissipation, high-resolution temperature sensors may be used, provided the temperature-density relationship is known, e.g. from additional shipborne CTD profiles (van Haren and Gostiaux 2012). The sensors are typically spaced at 1-m intervals over the entire 100-m-long mooring line and sample at a rate of 1 Hz. Thus, high-frequency internal waves (examples in Fig. 5.1 from the Llobregat prodelta), and especially also turbulent overturning (examples in Fig. 5.2 from the Ebro prodelta), can be detailed.

The time-scale of the largest overturns in Fig. 5.2a, b is 1000–1500 s. This is nearly equal to the buoyancy period observed in very thin (<2 m) stratified layers that border the

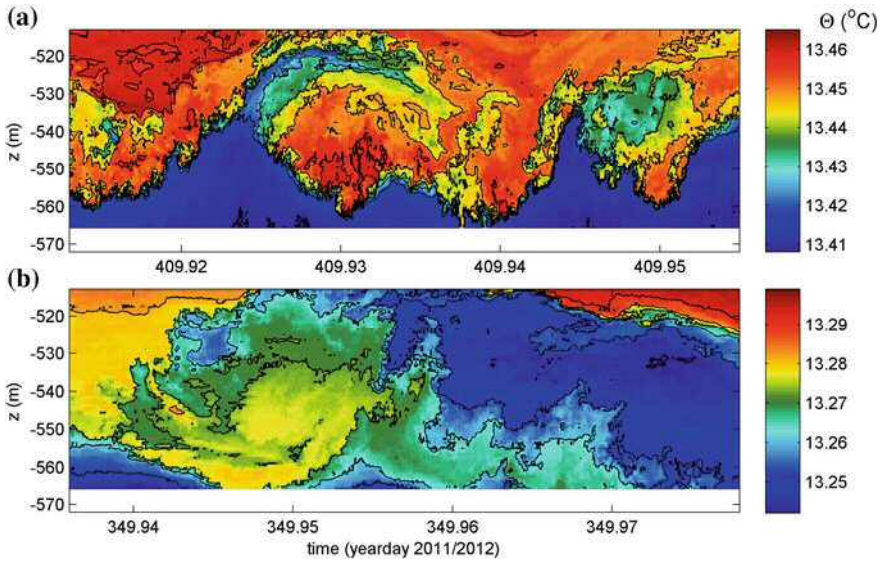

Fig. 5.2 One-hour examples of depth-time series of ~50 m vertical overturns observed using high-resolution temperature sensors above the continental slope in the Gulf of Valencia (after van Haren et al. 2013). *Both panels* have a temperature range of 0.062 °C and contours every 0.01 °C, but they differ in absolute values. **a** During strong downslope flow. **b** During upslope flow

overturns. The shear that drives these overturns varies locally on the buoyancy scale (reaching 9×10^{-3} s^{-1} over 20-m intervals for the period in Fig. 5.2a). It is superposed on a larger-scale shear of about 2×10^{-3} s^{-1} created by inertial motions and the sub-inertial Northern Current (van Haren et al. 2013).

From a single mooring with multiple instruments, one can measure the vertical internal wavelength $2\pi/m$, where m is the wavenumber, from the phase shift in a depth-time diagram. The horizontal wavelength $2\pi/k_h$, where k_h is the wavenumber, is found through the dispersion relation (e.g., LeBlond and Mysak 1978): $\sigma^2 = N^2k_h^2/(k_h^2 + m^2 + (N^2/2g)^2)$, where g denotes the acceleration of gravity.

5.4 Discussion

Despite the similarity in horizontal wavelength between sediment and internal waves, the need for scepticism is suggested by the fact that sediment waves take such a long time to grow compared with the time scales of internal waves. However, other frictional processes such as surface waves and the processes of near-inertial, tidal and boundary currents also have time scales that are far shorter than those of sand-ripple and sediment wave growth. In the deep sea, at depths greater than about 100 m above the steepest part of continental slopes, these frictional processes are less important than those induced by internal wave motions, in particular breaking. This is because observed overturns are not associated with friction on a rotating Earth as they do not comply with Ekman dynamics above sloping bottoms, which predicts greater turbulence for a downwelling-favourable along slope flow like the Northern Current in the NW Mediterranean.

When turbulent bores move up the slope, their peak currents far exceed those of other processes (both frictionally at the bottom and in the interior) that are important for sweeping material into suspension. However, a more comprehensive classification of internal wave breaking processes in relation to bedforms is still highly needed. Such a classification can only be made using detailed observations.

References

Armi, L. (1978). Some evidence for boundary mixing in the deep ocean, *J. Geophys. Res., 83*, 1971–1979.

Cacchione, D.A., and D.E. Drake (1986). Nepheloid layers and internal waves over continental shelves and slopes, *Geo-Mar. Lett., 16*, 147–152.

Hosegood, P., J. Bonnin, and H. van Haren (2004). Solibore-induced sediment resuspension in the Faeroe-Shetland Channel, *Geophys. Res. Lett., 31*, L09301, doi:10.1029/2004GL019544.

Klymak, J.M., and J.N. Moum (2003). Internal solitary waves of elevation advancing on a shoaling shelf, *Geophys. Res. Lett., 30*, 2045, doi:10.1029/2003GL017706.

Lamb, K.G. (2014). Internal wave breaking and dissipation mechanisms on the continental slope/shelf, *Ann. Rev. Fluid Mech., 46*, 231–254.

LeBlond, P.H., and L.A. Mysak (1978). *Waves in the Ocean*, 602 pp., Elsevier, New York.

McPhee-Shaw, E.E., and E. Kunze (2002). Boundary-layer intrusions from a sloping bottom: A mechanism for generating intermediate nepheloid layers, *J. Geophys. Res. 107*, doi:10.1029/2001JC000801.

Munk, W., and C. Wunsch (1998). Abyssal recipes II: Energetics of tidal and wind mixing, *Deep-Sea Res. I, 45*, 1977–2010.

Puig, P., A.S. Ogston, J. Guillén, A.M.V. Fain and A. Palanques (2007). Sediment transport processes from the topset to the foreset of a crenulated clinoform (Adriatic Sea), *Cont. Shelf Res., 27*, 452–474.

Ribó, M., et al. (2016). Large fine-grained sediment waves over the Valencia slope, *This book.*

Urgeles, R., et al. (2011). A review of undulated sediment features on Mediterranean prodeltas: distinguishing sediment transport structures from sediment deformation, *Mar. Geophys. Res., 32*, 49–69.

van Haren, H., and L. Gostiaux (2012). Detailed internal wave mixing observed above a deep-ocean slope, *J. Mar. Res., 70*, 173–197.

van Haren, H., M. Ribó, and P. Puig (2013). (Sub-)inertial wave boundary turbulence in the Gulf of Valencia, *J. Geophys. Res., 118*, 2067–2073, doi:10.1002/jgrc.20168.

van Haren, H., A. Cimatoribus, and L. Gostiaux (2015). Where large deep-ocean waves break, *Geophys. Res. Lett., 42*, 2351–2357, doi:10.1002/2015GL063329.

Verdicchio, G., and F. Trincardi (2006). Short-distance variability in slope bed-forms along the Southwestern Adriatic Margin (Central Mediterranean), *Mar. Geol., 234*, 271–292.

Vlasenko, V., and K. Hutter (2002). Numerical experiments on the breaking of solitary internal waves over a slope-shelf topography, *J. Phys. Oceanogr., 32*, 1779–1793.

Zhang, H.P., B. King and H.L. Swinney (2008). Resonant generation of internal wave on a model continental slope, *Phys. Rev. Lett., 100*, 244504.